



OPEN ACCESS

## ORIGINAL RESEARCH

# Wall enhancement ratio and partial wall enhancement on MRI associated with the rupture of intracranial aneurysms

Guang-xian Wang,<sup>1</sup> Li Wen,<sup>1</sup> Sheng Lei,<sup>1</sup> Qian Ran,<sup>1</sup> Jin-bo Yin,<sup>2</sup> Zi-li Gong,<sup>3</sup> Dong Zhang<sup>1</sup>

<sup>1</sup>Department of Radiology, Xinqiao Hospital, Third Military Medical University, Chongqing, China

<sup>2</sup>Department of Neurosurgery, Xinqiao Hospital, Third Military Medical University, Chongqing, China

<sup>3</sup>Department of Neurology, Xinqiao Hospital, Third Military Medical University, Chongqing, China

**Correspondence to**

Dr Dong Zhang, Department of Radiology, Xinqiao Hospital, Third Military Medical University, Chongqing 400037, China; xqzhangdong@163.com

Received 7 July 2017

Revised 21 August 2017

Accepted 28 August 2017

**ABSTRACT**

**Objectives** To evaluate the risk factors for rupture of intracranial aneurysms (IAs) using high resolution MRI (HRMRI).

**Methods** 91 consecutive patients with 106 IAs were reviewed from February 2016 to April 2017. Patients and IAs were divided into ruptured and unruptured groups. In addition to the clinical characteristics of the patients, the features of IAs (eg, shape) were evaluated by CT angiography, whereas wall thickness, enhanced patterns, and enhancement ratio (ER) were evaluated by MRI. Multiple logistic regression analysis was used to identify independent risk factors associated with the rupture of IAs. Receiver operating characteristic curve analysis was performed on the final model, and the optimal thresholds were obtained.

**Results** ER (OR 6.638) and partial wall enhancement (PWE) (OR 6.710) were not markers of aneurysms more prone to rupture, but simply were more commonly found in the ruptured aneurysm cohort. The threshold value for ER was 61.5%.

**Conclusions** ER ( $\geq 61.5\%$ ) and IAs with PWE are better predictors of rupture. Increased attentions should be paid to these factors during assessment of IA rupture.

arterial disease, including angiogram negative non-perimesencephalic subarachnoid hemorrhage,<sup>3</sup> atherosclerotic plaque, vasculitis, reversible cerebral vasoconstriction syndrome, moyamoya disease, and even IAs.<sup>4</sup> Aneurysmal wall enhancement (AWE) is believed to reflect wall inflammation and is a new imaging biomarker for risk evaluation.<sup>5–12</sup> However, AWE has not been sufficiently investigated. We hypothesized that AWE might be a marker of aneurysmal wall inflammation as well as inflammation associated with rupture of IAs and, therefore, the enhancement ratio (ER) of AWE would be stronger in ruptured IAs (RIAs) than in UIAs.

**MATERIALS AND METHODS****Patients**

This retrospective study was approved by our institutional ethics committee. From February 2016 to April 2017, 106 patients with saccular IAs diagnosed by CT angiography (CTA) were recruited to undergo enhanced HMRM. Exclusion criteria included the following: (1) children, pregnancy and patients who had contraindications to MRI and the use of contrast agents, such as patients with a pacemaker, claustrophobia, renal insufficiency, or contrast allergy (n=2); (2) patients with traumatic fusiform IAs, cases in which arteriovenous malformations were present, and cases with poor image quality (n=4); (3) patients with a recent history of aspirin or non-steroidal anti-inflammatory drug use (n=3); and (4) patients with RIAs who experienced a serious disturbance of consciousness or those who were unable to cooperate during the MRI examination (n=6). Finally, 91 patients (19 with RIAs and 72 with UIAs) with 106 IAs (19 RIAs and 87 UIAs) were available for analysis. Eighteen RIAs and 30 UIAs were managed with either coiling or clipping, and 58 UIAs were observed. Between follow-ups with CTA or MR angiography (MRA) (mean time 8.3 months, range 3–15 months), one aneurysm ruptured and was classified in the ruptured group, 7 patients with 8 IAs were lost (lost track of or died), and the remainder of the IAs did not rupture. The patients' clinical data were extracted from hospital medical records. In cases of multiple IAs, the RIAs were determined based on CT, angiographic, or operative findings.

**CT angiography**

CTA was performed on a 64 slice CT machine (GE LightSpeed VCT; GE Healthcare, Wisconsin, USA).



CrossMark

**To cite:** Wang G, Wen L, Lei S, et al. *J NeuroIntervent Surg* Published Online First: [please include Day Month Year]. doi:10.1136/neurintsurg-2017-013308



**Figure 2** A middle-aged woman presented with headache due to a right-sided M1–M2 unruptured aneurysm (A). Post-contrast MRI (C) indicates entire wall enhancement (arrows) compared with the pre-contrast image (B).

Three-dimensional volume rendered (VR) images were then obtained after contrast agent (Visipaque 320; GE Healthcare) injection at a rate of 4–4.5 mL/s.

#### Magnetic resonance imaging

MR was performed using a 3.0 T clinical MR scanner (Signa HDx, GE Healthcare) with an 8 channel head coil. The examination protocol included three-dimensional time of flight MRA, and pre- and post-contrast T1WI HRMRI. First, a three-dimensional time of flight MRA was performed for the localization of subsequent scans. The imaging time was approximately 3 min 42 s and the images generated were three-dimensional VR with maximum intensity projection. Then, the walls of the IAs were imaged by a two-dimensional black blood T1WI FSE sequence before and after contrast agent administration. The imaging parameters optimized for the T1W sequence were as follows: TR/TE=580/11 ms, field of view=16×16 cm, acquired matrix=384×224, slice thickness=1.2 mm, and layer spacing=0 mm. A total of 20 mL of Gd-BOPTA (MultiHance; Bracco, Shanghai, China) was injected into the antecubital vein by an automatic injector (Medrad; Warrendale, Pennsylvania, USA) at a rate of 2 mL/s. Each aneurysm scan was performed in the axial, coronal, sagittal, and axial planes in turn, and no patient had contrast allergy. The total scan time was 3 min 8 s per sequence.

#### Image analysis

All images were transferred to the GE Advantix workstation (Advantage Windows 4.5) and image analysis was performed by two experienced radiologists (LW, 18 years' experience in neuroradiology; SL, 5 years' experience in vascular imaging). For CTA image analysis, the images were reconstructed into a three-dimensional VR model for each aneurysm; then, the observers found the best viewing angle at which to measure the morphological indices of the IAs, including neck width (the largest cross sectional diameter of the aneurysm neck), depth

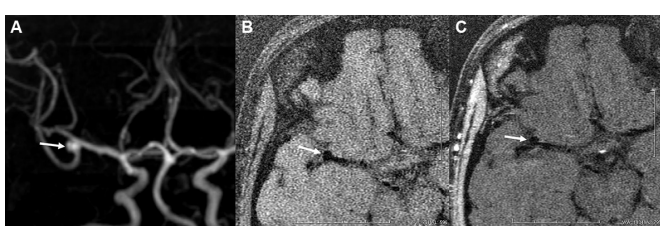


**Figure 1** Frontal projection of maximum intensity projection shows a right-sided M1–M2 unruptured aneurysm in a middle-aged woman (A). Post-contrast MRI (C) indicates no enhancement of the aneurysmal wall (arrows) compared with the pre-contrast image (B).

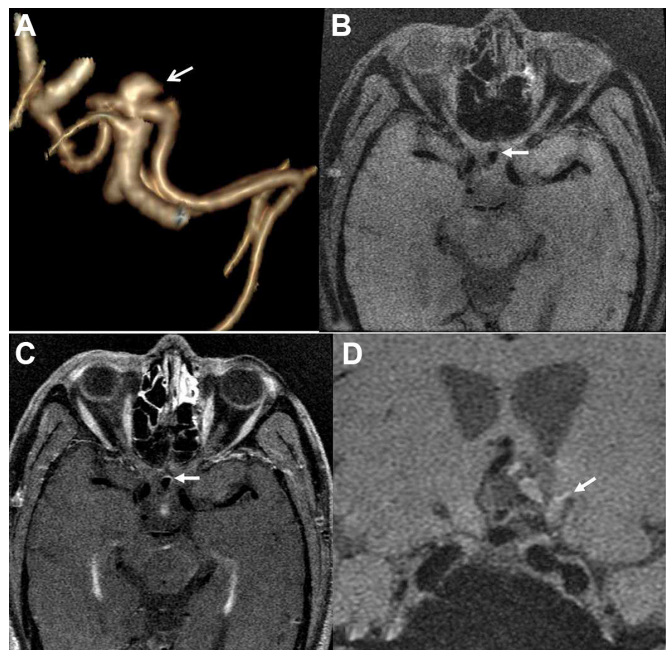


**Figure 3** A middle-aged man presented with headache due to an aneurysm in the anterior communicating artery. Three-dimensional volume rendering (VR) by CT angiography shows the irregular shape of the aneurysm (arrow) (A). Post-contrast MRI (C) indicates partial wall enhancement (arrows) compared with the pre-contrast image (B). Nineteen days later, the aneurysm ruptured with subarachnoid hemorrhage (arrow) (D).

(the longest diameter between the neck and dome), maximum size (the largest measurement in terms of maximum dome diameter or width), and flow angle (angle between the vector of depth of the aneurysm and the vector of the centerline of the parent artery), as well as location, bifurcation (or not), and shape (simple lobed or irregular). The location of the IAs was categorized as anterior circulation or posterior circulation. These variables have previously been identified and depicted in the literature.<sup>13 14</sup> For MR image analysis, the observers determined the enhanced patterns, ER, and wall thickness of the IAs. The wall enhancement patterns were categorized as no (no enhancement of the wall compared with pre-contrast scan), entire (the whole wall presented as enhanced) or partial wall enhancement (PWE, only part of the wall presented as enhanced) (figures 1–3).<sup>8 9 11</sup> The signal intensity (SI) at the neck, body, and dome portions of the IAs was measured manually on the pre- and post-enhancement images, magnified three-fold on the PACS system (figure 4). Then, average values were used, and the maximum SI was chosen out of four enhancement sequences. ER was calculated as follows:  $ER = (\text{SI}_{\text{max}} - \text{SI}_{\text{pre}})/\text{SI}_{\text{pre}} \times 100\%.$ <sup>15</sup> Wall thickness at the neck, body, and dome portions of the IAs was measured manually on the post-enhancement images. Average values were used for all subsequent statistical analyses.

#### Statistical analysis

All statistics were performed using the Statistical Package for Social Sciences (SPSS, Illinois, USA, V17.0), and a p value <0.05 was considered statistically significant. All data are expressed as means±SD or n (%), as appropriate.  $\chi^2$  tests and paired t tests or Mann–Whitney U tests were used to determine the reliability of the numerical data of the two observers. For continuous data, a two tailed independent Student's t test (for normally distributed

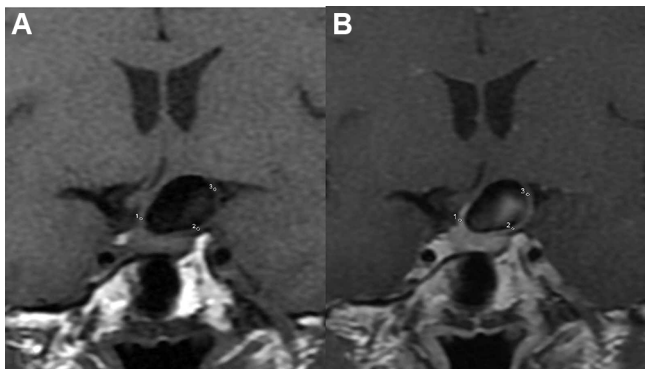


**Figure 4** Signal intensity at the neck, body, and dome portions of the intracranial aneurysms was measured manually on the pre- (A) and post-enhancement (B) images. The signal intensity values were determined in circular regions of interest placed in the aneurysm wall, and average values were used.

data) or the Mann–Whitney U test (for non-normally distributed data) was performed. Categorical data were compared using  $\chi^2$  tests. All variables were entered into univariate analysis if p values were  $<0.2$ . Those features achieved significance in univariate analysis ( $p<0.05$ ) were entered into forward multiple logistic regression to calculate OR and 95% CI for the likelihood of aneurysm rupture. Receiver operating characteristic (ROC) curve analysis was performed to determine the cut-off value, and the criterion for the selection of the cut-off point was when the value of (sensitivity + specificity – 1) reached its maximum.

## RESULTS

Clinical characteristics of the 91 patients are listed in **table 1**. Of these patients, 62 were women and 29 were men (2.1:1 ratio of women to men). Mean age of the patients was  $56.76 \pm 9.91$  years ( $55.21 \pm 12.11$  years for patients with RIAs and  $57.17 \pm 9.20$  years for patients with UIAs). Fifty-six years was chosen to dichotomize the sample as mean patient age was 56.76 years. According to the  $\chi^2$  test, no associations were found between clinical characteristics and rupture of IAs.

The level of agreement between the two observers with respect to the morphological data was satisfactory ( $p>0.05$ ). The geometric and morphological characteristics of RIAs and UIAs are shown in **table 2**. IAs with an irregular shape, no

**Table 2** Morphological characteristics of aneurysms

| Morphologic parameter        | Unruptured (n=87)  | Ruptured (n=19)    | p Value |
|------------------------------|--------------------|--------------------|---------|
| Anterior circulation (n (%)) | 85 (97.7)          | 19 (100.0)         | 1.000   |
| Bifurcation (n (%))          | 37 (42.5)          | 12 (63.2)          | 0.102   |
| Irregular shape* (n (%))     | 35 (40.2)          | 16 (84.2)          | 0.001   |
| Neck width (mm)              | $4.56 \pm 1.80$    | $4.46 \pm 1.99$    | 0.835   |
| Depth (mm)*                  | $5.99 \pm 6.04$    | $7.02 \pm 4.33$    | 0.002   |
| Maximum Size (mm)*           | $7.29 \pm 6.60$    | $8.34 \pm 4.78$    | 0.009   |
| Flow angle (°)               | $113.02 \pm 28.71$ | $113.30 \pm 28.22$ | 0.969   |
| Wall thickness (mm)*         | $0.93 \pm 0.47$    | $1.17 \pm 0.34$    | 0.001   |
| Enhanced patterns (n (%))    |                    |                    |         |
| No*                          | 23 (26.4)          | 0 (0.0)            | 0.011   |
| Entire                       | 57 (65.2)          | 10 (52.6)          | 0.291   |
| Partial*                     | 7 (8.0)            | 9 (47.4)           | <0.001  |
| Enhanced ratio (%)*          | $0.63 \pm 0.70$    | $0.90 \pm 0.45$    | <0.001  |

\*Variables showing significant difference by univariate analysis ( $p<0.05$ ).

enhancement, PWE, depth, maximum size, wall thickness, and ER were associated with rupture.

Then, these variables ( $p \leq 0.05$ ) were entered into a forward conditional multiple logistic regression model. The ER (OR 6.638) and IAs with PWE (OR 6.710) were better predictors of rupture (**table 3**).

The threshold value of the ER was 61.5%, and the value of the area under the curve was 0.798 (**figure 5**); sensitivity and specificity values for the detection of ruptured aneurysms were 89.5% and 63.2%, respectively (**table 4**).

## DISCUSSION

Several experimental and human studies have suggested that inflammation is a key component in the pathophysiology of the formation and rupture of IAs.<sup>5 16 17</sup> The pathobiological alterations in the aneurysm wall are very complicated and have been shown to involve many histopathologic changes, including disruption of the internal elastic lamina, smooth muscle cell migration, myointimal hyperplasia,<sup>18</sup> intramural bleeding from the fragile vasa vasorum or atherosclerosis, infiltration of inflammatory cells, and release of inflammatory cytokines and proteases.<sup>10 19</sup> These processes then destroy the extracellular matrix proteins and weaken the vessel wall.<sup>10</sup> Previous studies have used ultra small particles of iron oxide as an MRI specific target

**Table 1** Clinical characteristics of patients with aneurysms

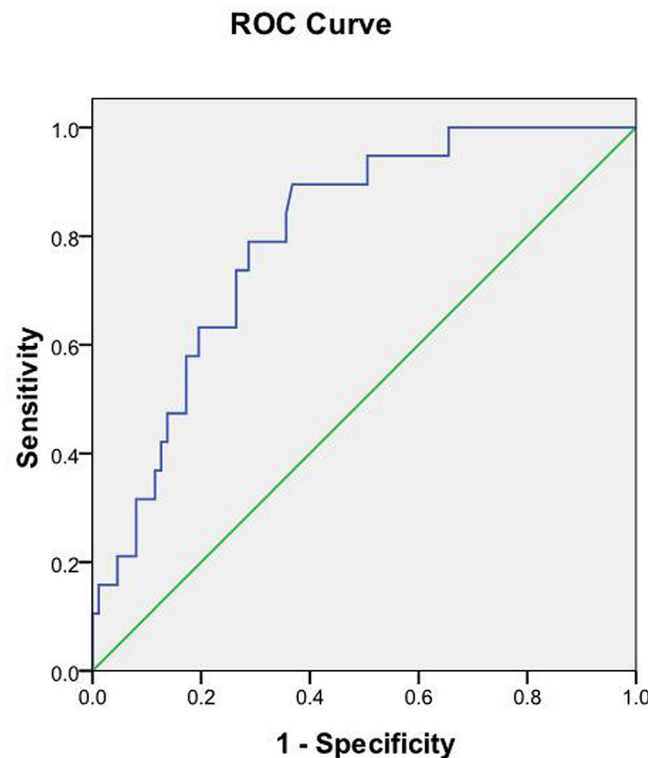
| Characteristic           | Unruptured (n=72) | Ruptured (n=19) | p Value |
|--------------------------|-------------------|-----------------|---------|
| Men (n (%))              | 22 (30.6)         | 7 (36.8)        | 0.601   |
| Age( $\geq 56$ years)    | 41 (56.9)         | 9 (47.4)        | 0.836   |
| Hypertension             | 31 (43.1)         | 9 (47.4)        | 0.736   |
| Heart disease            | 7 (9.7)           | 2 (10.5)        | 1.000   |
| Diabetes mellitus        | 5 (6.9)           | 1 (5.3)         | 1.000   |
| Cerebral atherosclerosis | 15 (20.8)         | 3 (15.8)        | 0.867   |
| Current alcohol          | 11 (15.3)         | 3 (15.8)        | 1.000   |
| Current smoking          | 13 (18.1)         | 4 (21.1)        | 1.000   |
| Multiple aneurysms       | 8 (11.1)          | 2 (10.5)        | 1.000   |

Values are n (%).

**Table 3** Binary logistic regression analysis for all ruptured aneurysms

| Variable            | OR    | p Value | 95%CI           | $\beta$ |
|---------------------|-------|---------|-----------------|---------|
| Partial enhancement | 6.710 | 0.004   | 1.805 to 24.938 | 1.904   |
| Enhancement ratio   | 6.638 | 0.003   | 1.919 to 22.967 | 1.893   |

$\beta$ , partial regression coefficient.



Diagonal segments are produced by ties.

**Figure 5** Area under the receiver operating characteristic (ROC) curve for the enhancement ratio (ER) is 0.798 (95% CI 0.703 to 0.893). The cut-off point for the ER is 61.5%, with sensitivity 89.5% and specificity 63.2%.

contrast agent of inflammation, but this is difficult to implement in routine clinical practice.<sup>5,6</sup> Recently, HRMRI has been used in individuals with IAs, and AWE was considered to be a sign of wall inflammation, although this still requires further investigation. In this study, we evaluated the wall of IAs using the black blood sequence and a common gadolinium agent, and found that the ER and PWE are associated with rupture of IAs.

AWE on HRMRI has already been found to be an important indicator of an unsteady state and rupture.<sup>7–12</sup> Previous studies have reported that AWE was seen more frequently in RIAs,<sup>7,8,11</sup> defined AWE as non-evident, faint, or strong, and indicated that strong enhancement has a high specificity for RIAs.<sup>8</sup> However, this evaluation method sometimes leads to a dilemma—for example, sometimes distinguishing faint from strong enhancement is difficult. In this study, we measured the wall SI on pre- and post-enhancement images and the quantitative method was employed to avoid these issues. We found that the ER ( $\geq 61.5\%$ ) correlated with rupture of IAs and with higher sensitivity than our previous studies by CTA.<sup>13,14</sup> However, no consensus exists with respect to a common threshold value, and this finding

also supports the idea that AWE would be stronger in RIAs than in UIAs. The reason for this may be the presence of more intense inflammation and increased permeability, intraluminal thrombus, stagnation, or leakage of the contrast agent on strong wall enhancement.

Previous studies have reported that AWE may be a helpful finding for identification of RIAs in patients with multiple IAs and subarachnoid hemorrhage<sup>8</sup> and may be suggestive of the rupture point.<sup>8,11</sup> In this study, the partially enhanced apex of 6 RIAs coincided with the ruptured point, as determined by HRMRI or during surgery. Our data showed that one unruptured aneurysm with PWE ruptured 19 days later. Therefore, the PWE of an IA may suggest the rupture point, which is helpful information for clinicians.

In fact, 16 IAs with PWE were included in our study, and all of the enhancement was present in the irregularly shaped portion or in daughter sacs. Furthermore, 16 RIAs had an irregular shape, and 9 RIAs exhibited PWE. Our previous studies reported that IAs with an irregular shape were associated with a higher risk of rupture.<sup>13,14</sup> The reason for this may be that the irregular shape leads to instability of the blood flow pattern, induction of damage in the endothelial cell layer, inflammatory cell infiltration, thin walls and dense areas in the vasa vasorum, as well as increased permeability, stagnation, or leakage of the contrast agent.<sup>8,9,18</sup> All of these can lead to PWE.

The rupture point of the aneurysm is usually in the dome portion, and thin walls are positively correlated with the rupture of IAs. A previous study also reported that the thickness of the aneurysmal wall was greater in the neck portion than in the dome portion.<sup>20</sup> We also measured wall thickness and, interestingly, the wall thickness of RIAs was greater than that of UIAs. The reasons for this conflicting result may be that we measured wall thickness on post-enhancement images and that the wall we visualized was the true wall plus other tissue components, such as adjacent parenchyma or leakage of the contrast agent. Another reason is that we may have overestimated wall thickness due to the partial volume effects.<sup>21</sup> Hence we suggest that enhanced wall thickness should be excluded as a predictor of rupture risk of IAs.

We also investigated the clinical characteristics of the patients, such as age and occurrence of cerebral atherosclerosis. Our previous studies have reported that these factors were associated with rupture.<sup>13,14,12,13</sup> However, in this study, the results showed that these clinical factors were not significantly different between RIAs and UIAs. The reason for this may be that this study had a relatively small sample size.

### Limitations

This study had several limitations. First, the data were collected from a single relatively small center. Second, this was a retrospective study, and thus the size of the RIAs may have changed and generated inflammatory changes around the wall of the IAs due to rupture, although a previous study reported that aneurysms size does not shrink after rupture.<sup>22</sup> Third, the researchers performing the measurements were not completely blinded to the fact that the aneurysms were ruptured or unruptured, and this may have resulted in bias. Fourth, subarachnoid hemorrhage from a ruptured IA could generate an inflammatory response around the wall, which may give false positive results. However, a previous study reported that AWE might precede rupture rather than occur as a result of rupture.<sup>4</sup> Fifth, the HRMRI resolution was not sufficiently high to precisely measure the wall, especially wall thickness  $< 1$  mm, and there may have been considerable inter/inter-rater reliability. Finally, we did not investigate the relationship between ER and the degree of inflammation by

**Table 4** Area under the curve for enhancement ratio

| Characteristic    | Area  | Threshold value (%) | p Value | Sen (%) | Spe (%) | 95% CI         |
|-------------------|-------|---------------------|---------|---------|---------|----------------|
| Enhancement ratio | 0.798 | 61.5                | <0.001  | 89.5    | 63.2    | 0.703 to 0.893 |

Sen, sensitivity; Spe, specificity; Threshold value, the cut-off for the enhancement ratio.

pathology because it is difficult to obtain pathology results. In the future, larger sample sizes and a prospective study should be conducted, and we would expect to follow patients with untreated IAs for several years to observe the patterns of wall enhancement, degree of enhancement, and whether rupture occurs, although this could be very difficult. In addition, the relationship between ER and degree of inflammation requires confirmation in future animal studies. These are under our investigation.

## CONCLUSION

Based on the HRMRI findings, we found that ER ( $\geq 61.5\%$ ) and IAs with PWE were more commonly found in the ruptured aneurysm cohort. Thus, in clinical practice, greater attention should be paid to IAs with these characteristics.

**Acknowledgements** We thank American Journal Experts (AJE) for assisting in the preparation of this paper. We thank Ru-fu Xu, Professor of Epidemiology, Xinqiao Hospital, Third Military Medical University, for statistical advice.

**Contributors** Conceptualization: DZ. Data curation: LW. Investigation: SL, QR, J-bY, Z-IG. Methodology: DZ. Writing original draft: G-xW.

**Funding** The study was supported by the Research Project of the Third Military Medical University (2016YLC22).

**Competing interests** None declared.

**Patient consent** Obtained.

**Ethics approval** The study was approved by our institutional ethics committee (Xinqiao Hospital, 2016031).

**Provenance and peer review** Not commissioned; externally peer reviewed.

**Open Access** This is an Open Access article distributed in accordance with the Creative Commons Attribution Non Commercial (CC BY-NC 4.0) license, which permits others to distribute, remix, adapt, build upon this work non-commercially, and license their derivative works on different terms, provided the original work is properly cited and the use is non-commercial. See: <http://creativecommons.org/licenses/by-nc/4.0/>

© Article author(s) (or their employer(s) unless otherwise stated in the text of the article) 2017. All rights reserved. No commercial use is permitted unless otherwise expressly granted.

## REFERENCES

- Wiebers DO, Whisnant JP, Huston J, et al. Unruptured intracranial aneurysms: natural history, clinical outcome, and risks of surgical and endovascular treatment. *Lancet* 2003;362:103–10.
- Schneiders JJ, Marquerig HA, van Ooij P, et al. Additional value of intra-aneurysmal hemodynamics in discriminating ruptured versus unruptured intracranial aneurysms. *AJNR Am J Neuroradiol* 2015;36:1920–6.
- Coutinho JM, Sacho RH, Schaafsma JD, et al. High-resolution vessel wall magnetic resonance imaging in angiogram-negative non-perimesencephalic subarachnoid hemorrhage. *Clin Neuroradiol* 2017;27:175–83.
- Mandell DM, Mossa-Basha M, Qiao Y, et al. Intracranial vessel wall MRI: principles and expert consensus recommendations of the American society of neuroradiology. *AJNR Am J Neuroradiol* 2017;38:218–29.
- Hasan D, Chalouhi N, Jabbour P, et al. Early change in ferumoxytol-enhanced magnetic resonance imaging signal suggests unstable human cerebral aneurysm: a pilot study. *Stroke* 2012;43:3258–65.
- Hasan DM, Mahaney KB, Magnotta VA, et al. Macrophage imaging within human cerebral aneurysms wall using ferumoxytol-enhanced MRI: a pilot study. *Arterioscler Thromb Vasc Biol* 2012;32:1032–8.
- Matouk CC, Mandell DM, Günel M, et al. Vessel wall magnetic resonance imaging identifies the site of rupture in patients with multiple intracranial aneurysms: proof of principle. *Neurosurgery* 2013;72:492–6.
- Nagahata S, Nagahata M, Obara M, et al. Wall enhancement of the intracranial aneurysms revealed by magnetic resonance vessel wall imaging using three-dimensional turbo spin-echo sequence with motion-sensitized driven-equilibrium: a sign of ruptured aneurysm? *Clin Neuroradiol* 2016;26:277–83.
- Edjlali M, Gentric JC, Régent-Rodriguez C, et al. Does aneurysmal wall enhancement on vessel wall MRI help to distinguish stable from unstable intracranial aneurysms? *Stroke* 2014;45:3704–6.
- Liu P, Qi H, Liu A, et al. Relationship between aneurysm wall enhancement and conventional risk factors in patients with unruptured intracranial aneurysms: A black-blood MRI study. *Interv Neuroradiol* 2016;22:501–5.
- Hu P, Yang Q, Wang DD, et al. Wall enhancement on high-resolution magnetic resonance imaging may predict an unsteady state of an intracranial saccular aneurysm. *Neuroradiology* 2016;58:979–85.
- Bhogal P, Uff C, Makalanda HL. Vessel wall MRI and intracranial aneurysms. *J Neurointerv Surg* 2016;8:1160–2.
- Wang GX, Zhang D, Wang ZP, et al. Risk factors for the rupture of bifurcation intracranial aneurysms using CT angiography. *Yonsei Med J* 2016;57:1178–84.
- Wang GX, Yu JY, Wen L, et al. Risk factors for the rupture of middle cerebral artery bifurcation aneurysms using CT angiography. *PLoS One* 2016;11:e0166654.
- Zhong Y, Wang H, Shen Y, et al. Diffusion-weighted imaging versus contrast-enhanced MR imaging for the differentiation of renal oncocyomas and chromophobe renal cell carcinomas. *Eur Radiol* 2017 (Epub ahead of print : 19 Jun 2017).
- Chalouhi N, Ali MS, Jabbour PM, et al. Biology of intracranial aneurysms: role of inflammation. *J Cereb Blood Flow Metab* 2012;32:1659–76.
- Sawyer DM, Amenta PS, Medel R, et al. Inflammatory mediators in vascular disease: identifying promising targets for intracranial aneurysm research. *Mediators Inflamm* 2015;2015:1–10.
- Vakil P, Ansari SA, Cantrell CG, et al. Quantifying intracranial aneurysm wall permeability for risk assessment using dynamic contrast-enhanced MRI: A pilot study. *AJNR Am J Neuroradiol* 2015;36:953–9.
- Hasan D, Hashimoto T, Kung D, et al. Upregulation of cyclooxygenase-2 (COX-2) and microsomal prostaglandin E2 synthase-1 (mPGES-1) in wall of ruptured human cerebral aneurysms: preliminary results. *Stroke* 2012;43:1964–7.
- Park JK, Lee CS, Sim KB, et al. Imaging of the walls of saccular cerebral aneurysms with double inversion recovery black-blood sequence. *J Magn Reson Imaging* 2009;30:1179–83.
- Steinman DA, Antiga L, Wasserman BA. Overestimation of cerebral aneurysm wall thickness by black blood MRI? *J Magn Reson Imaging* 2010;31:766.
- Rahman M, Ogilvy CS, Zipfel GJ, et al. Unruptured cerebral aneurysms do not shrink when they rupture: multicenter collaborative aneurysm study group. *Neurosurgery* 2011;68:155–61.